Design and Implementation of Microwave Dual-Band Pass Interdigital Filter Using an Analytical Approach

Moutaz Albik [1] , Fariz Abboud[1] , Alaaeddin Sarhan[2] , Assal Alkhoder[2]
[1]Damascus University, Damascus, Syria
[2]Higher Institute of Applied Sciences and Technology, Damascus, Syria
albaikmotez1@gmail.com, f.abboud20@gmail.com, alaa.sarhan@hiast.edu.sy, a-alkhoder@hotmail.com

Abstract— **In this paper, benefiting from frequency transformation between the normalized frequency domain of low-pass prototype frequencies and the real frequency domain of the filter, a purely analytical procedure for dual-band filter design is used. The coupling matrix of the filter is analytically extracted, without the need to perform numerical optimization. The procedure also includes finding the equivalent circuit for these types of filters. The frequency transformation formula is verified through an example. The equivalent circuit and the coupling matrix are also analytically deduced through the same example. Using an electromagnetic structure simulator, an interdigital dual-band filter is designed and simulated. The simulation results fulfill the specifications of the given filter example, and the simulation results verify the possibility of achieving the required specifications of the filter frequency response. The designed and simulated filter has been implemented and measured using a Scalar Network Analyzer. The measurement results confirm the simulation results and the efficiency of the synthesis procedure.**

Index Terms— dual-band filter, dual-resonance frequency, frequency transformation, interdigital filter.

I. INTRODUCTION

Since the giant development revolution of modem telecommunication systems, the demand for multi-standard devices has considerably increased [1]. In order to follow the developing needs of customers, different frequency bands are reserved for different standards. Therefore, in order to incorporate two or more desired communication bands in a single hardware unit, or to reject unwanted interfering frequencies, multi band filters are needed. Multi-band filters are attracting more and more interest in modern microwave filters design [2]-[8].

The design of dual- or multi-band filters has been encountered in two classes of methods. The first class depends on filtering functions, where the filtering function is constructed based on polynomials [9]. While the second most prevalent class relies on frequency transformation techniques [10]. The second class methods have been developed based on Zolatarev function [11], [12], but this approach does not allow controlling the attenuation between the two pass bands (the stop band). This type of filters can be synthesized analytically by positioning technique of transmission poles and zeros [9], [13], [14]. However, this technique depends on numerical optimization procedures [15], as the

convergence may not be guaranteed; its efficiency can be subject to question or doubt (especially, in cases where high frequency selectivity is required). Another technique for designing dual-band bandpass filters (DBPF), is to cascade a wide-band filter with a band-stop one [16], but this design gives a large filter size.

In [17], the authors presented a method for designing a symmetric DBPF filter, in which the frequency response is symmetric with respect to a frequency within the stop band. Whereas, in [18], two approaches were presented to design dual-band microwave filters, by creating transmission zeros and placing them within the required stop band. The first method resulted in a symmetrical response (the two pass bands had the same width, and the transmission zeros were placed symmetrically within the stop band), while the response in the second method was asymmetric (the two pass bands had different widths, and the transmission zeros were located at the same frequency in the stop band). Both methods depend on frequency transformation and the well-known prototype synthesis technique [20], [21], and the implementation in [18] relies on coupled resonant cavities. In [19], authors proposed the technique of synthesis and design of dual- and triple-band filters with symmetric Chebyshev and Elliptic frequency responses using substrate integrated waveguide technology. While authors, in [20], focused on the method of synthesis, design and how to create the stop band using transmission zeros by connecting resonators, which are responsible for transmission zeros in the stop band, where microstrip transmission line technology was used in designing some examples to verify the synthesis method.

A method for constructing a triple band filter based on the frequency transformation between the normalized frequency domain and the real one is presented in [19]. Where, new topologies containing cross-coupling have been proposed. According to this method, coupling coefficients and external quality factors can be analytically calculated. In order to verify the theoretical synthesis method, the authors designed and implemented a triple band filter with microstrip line technology.

In all of the above methods for filter synthesis, a coupling matrix representing the coupling coefficients between the filter resonators (including the resonators responsible for the stop bands or the cross-coupling coefficients) is obtained.

In this article, we propose to design a dual-band interdigital filter. For this purpose, we suggest to use the frequency transformation method to synthesize the dual-band filter, where this transformation is applied on the low-pass prototype in order to obtain coupled resonators of the filter (we call them primary resonators or band-pass resonators) in the form of inline coupled resonators, each of them is connected with a new resonator, where, these new resonators are responsible for placing the transmission zeros within the stop band, with no cross-coupling between the inline coupled resonators. This method constitutes an accurate approach to obtain the coupling matrix from the required characteristics of the filter, namely: filter degree and return loss or ripple in the pass band in addition to the frequencies at the edges the pass bands of the desired filter's response. Waveguide technology for designing these types of filters has been proposed in some scientific publications [2], [6].

Combline technology was also proposed in some scientific publications [9], [18], but the proposal in [18] required cross-coupling between the inline filter resonators, which increases the complexity of the structure, while in [9] two topologies were proposed using combline resonators, one of them also adopts cross-coupling, in this method and the method proposed in [18], the structure of the coupling matrix needs numerical optimization. As for the second method in [9], it used dual-mode resonators, but the coupling between the two resonance modes, which is responsible for the stop band, is restricted by the geometrical dimensions of the resonators, which, in its turn, adds restrictions on the achievable specifications of the filter, especially in terms of the width of the stop band. In this article, we propose the use of interdigital resonator filter technique to design a dual-band filter. This technology allows obtaining wider ranges of coupling values between the main primary resonators and the stop band ones.

In section II, the synthesis technique of dual-band filter is described step by step. Synthesis procedure verification is shown in section III through an example for a filter design and simulation. The designed and simulated filter is implemented and measured. The measurement results are presented in section IV. In section V, conclusion remarks about the design procedure and the designed, simulated and implemented filter are shown.

II. DUAL-BAND FILTER SYNTHESIS TECHNIQUE

The used methodology, described in this section, provides a method that enables to design a dual-band filter using an analytic synthesis procedure. This procedure is inspired in [17], [19]. What distinguishes this technique from others is that it produces arbitrary asymmetric frequency domains and controls the location of the stop band without using numerical optimization on the coupling matrix. According to this synthesis technique, the so-called interim parameters (resonant frequency and susceptance slope parameter for each resonator) are derived directly from the edges of the required pass bands. These interim parameters along with some values from the low-pass prototype are sufficient to calculate the design parameters of the filter (the coupling matrix and external Q factors). This analytical method is more effective than the optimization methods.

The synthesis procedure consists of three main steps: the first step is to synthesize a low-pass prototype with a response of some type (an all-pole Chebyshev response is chosen in our example). The second step is to apply the frequency transformation between the low-pass prototype domain to the dual band one (this transformation is denoted by $D(\omega)$) which maps the response of the de-normalized dual band frequency domain to the normalized or the low-pass prototype domain. The third step is to find the coupling matrix for the filter. Depending on the procedure of synthesis, the synthesis can be validated by the response obtained from the coupling matrix, from the filter itself or using the electrical circuit model of the filter.

A. Step One: Low-Pass Prototype

In this study, a low-pass prototype with a Chebyshev response is chosen. The filter response is

characterized by the filter degree n and the ripple factor ε given by [20]:

$$\varepsilon = \sqrt{10^{\frac{L_{Ar}}{10}} - 1} \, , \tag{1}$$

where L_{Ar} (dB) ($L_{Ar} > 0$) is the ripple within the passband, and related to the return loss RL (dB) ($RL < 0$) as [20]:

$$L_{Ar} = -10 \, \log_{10}\left(1 - 10^{\frac{RL}{10}}\right) . \tag{2}$$

The transmission coefficient S_{21} and the return loss S_{11} are given by [20]:

$$|S_{21}(j\Omega)|^2 = \frac{1}{1 + \varepsilon^2 \cdot T_n^2(\Omega)} \, , \tag{3}$$

$$|S_{11}|^2 + |S_{21}|^2 = 1 \, , \tag{4}$$

where Ω is the normalized frequency and T_n is the Chebyshev function given by [20]:

$$T_n(\Omega) = \begin{cases} \cos\left(n \cdot \cos^{-1}\Omega\right) & |\Omega| \leq 1 \\ \cosh\left(n \cdot \cosh^{-1}\Omega\right) & |\Omega| > 1 \end{cases} . \tag{5}$$

Fig. 1.a shows an example of a 5th order low-pass prototype response with a return loss of -20 dB. Fig. 1.b shows the shape of the response and the ripple within the pass band, which is approximately equal to 0.0436 dB. We will use these values in the example explained in the following sections of this article.
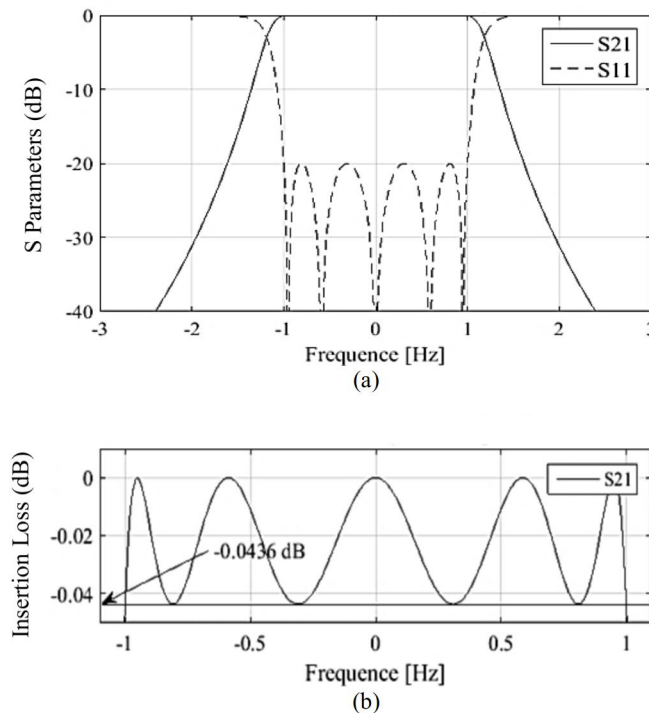

Fig. 1. 5th order low pass prototype response with $RL = -20$ dB
(a) The filter response (b) Zoom of filter's response in the pass band.

B. Step Two: Frequency Transformation

Frequency transformation is intended to obtain the response of the dual-band response from the low-pass prototype one. Fig. 2 shows this transformation.
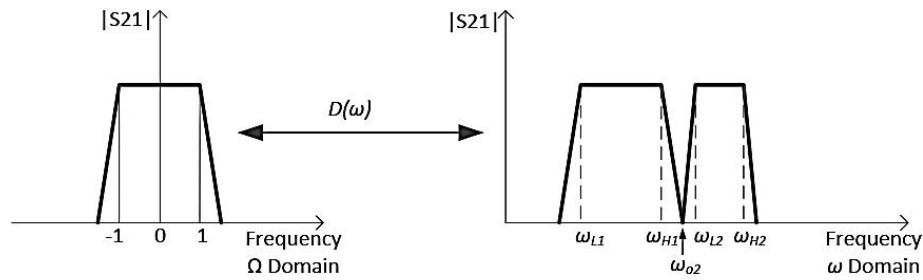
Fig. 2. Frequency transformation between low pass prototype response and dual-band one.

In Fig. 2, ω_{H1}, ω_{L1}, ω_{H2} and ω_{L2} are the edges of the first and second pass bands, and they represent the specification of the pass bands of the required filter. ω_{02} is the frequency of the transmission zeros between the two pass bands. In the synthesis technique, it is not necessary for the two pass bands to have the same width (i.e. the response might be asymmetric). However, both pass bands will have the same shape of the in- and out of-band response [21], where this dual band response is determined by the response of the low-pass prototype. The frequency transformation formula from the frequencies of the dual-band model or real frequencies to the frequencies of the low-pass prototype is given by the following formula [17]:

$$\Omega = b_1 \left(\frac{\omega}{\omega_{01}} - \frac{\omega_{01}}{\omega} \right) - \frac{1}{b_2 \left(\frac{\omega}{\omega_{02}} - \frac{\omega_{02}}{\omega} \right)} \, , \tag{6}$$

where, the interim parameters (b_1, ω_{01}, b_2 and ω_{02}) define the frequency transformation. It is noteworthy that, in addition to defining frequency transformation, these four parameters physically define all resonators in the proposed dual-band filter. b_1 and b_2 are the susceptance slope parameters and ω_{01} and ω_{02} are the resonance frequencies of the resonators. More details are provided in the following subsections.

The frequency transformation (given in (6)) maps the real frequency domain to the normalized one or the prototype frequency domain. However, the transformation required for the design must be in the opposite direction, i.e. from the normalized frequency domain (of the low-pass prototype) to the real frequency one. In order to perform this transformation, it is necessary first to obtain the interim parameters from the specifications of the pass bands, and then the inverse transformation of relation (6) can be found, i.e.:

$$\omega = D^{-1}(\Omega) \, . \tag{7}$$

Interim Parameters Extraction:

So in order to obtain the required transformation, we must first extract the interim parameters.

The extraction method of the relation between the interim parameters (b_1, ω_{01}, b_2 and ω_{02}) and the specifications of the filter pass bands (ω_{H1}, ω_{L1}, ω_{H2} and ω_{L2}) is referred in [17]. If we apply the frequency transformation formula (6), the lower edges of the pass bands ω_{L1} and ω_{L2} will be mapped from the real frequencies (de-normalized) to the frequency -1 in the domain of the normalized frequencies or the low-pass prototype frequencies, while the upper bounds ω_{H1} and ω_{H2} will be

mapped to the frequency $+1$ as shown in Fig. 2. Using relation (6), we can express:

$$D(-\omega_{L1}) = D(-\omega_{L2}) = D(\omega_{H1}) = D(\omega_{H2}) = 1. \tag{8}$$

Let's rewrite (6) as:

$$VD(\omega) = D(\omega) - 1 = \frac{ZD(\omega)}{PD(\omega)}, \tag{9}$$

where $ZD(\omega)$ and $PD(\omega)$ are polynomials of ω such that the coefficient of the highest power term in the numerator is one. That is, $D(\omega) - 1$ can be written as a fraction of two polynomials. Since this fraction tends to zero at ω_{H1}, ω_{L1}, ω_{H2} and ω_{L2}, these frequencies represent zeros for the numerator $ZD(\omega)$, which means that:

$$ZD(\omega) \equiv (\omega + \omega_{L1}) \cdot (\omega + \omega_{L2}) \cdot (\omega - \omega_{H1}) \cdot (\omega - \omega_{H2}) = 0. \tag{10}$$

Therefore, relation (10) can be expanded to obtain a polynomial of the fourth degree where the coefficient of the highest power term is one. So it takes the following form:

$$ZD(\omega) \equiv \omega^4 + z_3\omega^3 + z_2\omega^2 + z_1\omega^1 + z_0 = 0, \tag{11}$$

where z_i's depends on the bounds of the pass bands. They are given by:

$$z_3 = \omega_{L1} + \omega_{L2} - \omega_{H1} - \omega_{H2}, \tag{12}$$

$$z_2 = \omega_{L1} \cdot \omega_{L2} + \omega_{H1} \cdot \omega_{H2} - (\omega_{L1} + \omega_{L2}) \cdot (\omega_{H1} + \omega_{H2}), \tag{13}$$

$$z_1 = \omega_{H1} \cdot \omega_{H2} \cdot (\omega_{L1} + \omega_{L2}) - \omega_{L1} \cdot \omega_{L2} \cdot (\omega_{H1} + \omega_{H2}), \tag{14}$$

$$z_0 = \omega_{L1} \cdot \omega_{L2} \cdot \omega_{H1} \cdot \omega_{H2}. \tag{15}$$

Using (6), (9) can be rewritten by unifying the denominators and converting to a fraction where its numerator and denominator are polynomials, and after normalizing the numerator and denominator to the coefficient of the highest power term in the numerator, $ZD(\omega)$ can be written in terms of the interim parameters as:

$$ZD(\omega) \equiv \omega^4 + \left(-\frac{\omega_{01}}{b_1}\right)\omega^3 + \left(\omega_{01}^2 + \omega_{01}^2 + \frac{\omega_{01}\omega_{01}}{b_1 b_2}\right)\omega^2 + \left(\frac{\omega_{01}\omega_{02}^2}{b_1}\right)\omega + \frac{\omega_{01}\omega_{01}}{b_1 b_2} = 0. \tag{16}$$

Comparing between (11) and (16) gives:

$$\omega_{01} = \sqrt{-\frac{z_0 \cdot z_3}{z_1}}, \tag{17}$$

$$\omega_{02} = \sqrt{-\frac{z_1}{z_3}}, \tag{18}$$

$$b_1 = \sqrt{-\frac{z_0}{z_1 \cdot z_3}}, \tag{19}$$

$$b_2 = \frac{z_1 \cdot z_3^2}{z_1 \cdot z_2 \cdot z_3 + z_1^2 - z_0 \cdot z_3^2} \cdot \sqrt{-\frac{z_1}{z_3}}. \tag{20}$$

This way, the interim parameters are found in terms of the specification of the required pass bands

using a purely analytical way, where the values of z_i's are given by (12) to (15).

Frequency Transformation from the Normalized Frequency Domain to the Real one:

Having found the interim parameters, the inverse transformation that allows finding the response in the real frequency domain (i.e. the real filter response) from the normalized frequency domain response (or the low-pass prototype response) can be found, i.e. equation (7). For a dual-band filter, the inverse transformation is obtained by solving the quadratic equation that can be given from (6) by:

$$\omega^4 - \left(\frac{\Omega \cdot \omega_{01}}{b_1}\right)\omega^3 - \left(\omega_{01}^2 + \omega_{02}^2 + \frac{\omega_{01} \cdot \omega_{02}}{b_1 \cdot b_2}\right)\omega^2 + \left(\frac{\Omega \cdot \omega_{01} \cdot \omega_{02}^2}{b_1}\right)\omega + \left(\omega_{01}^2 \cdot \omega_{02}^2\right) = 0 . \quad (21)$$

This equation is solved using MATLAB. We will use MATLAB in order to verify the transformation formula through the given example in the following subsections.

C. Step Three: Finding the Coupling Matrix and the Equivalent Circuit

Consider a dual-band filter containing $2n$ resonators as shown in Fig. 3. Resonators from 1 to n are the inline band-pass resonators, and they all resonate at the frequency ω_{01}. Resonators from $n + 1$ to $2n$ are the resonators responsible for the stop-band (called band-stop resonators), and they all resonate at frequency ω_{02}. Therefore, there are n identical dual-resonance frequency resonators in the 2nd-degree dual-band filter. Each of these resonators constitutes the periodic unit of the dual-band filter, which can be considered as the building blocks of the structure [17]. For the dual-band filter topology, the used frequency transformation is given in (6); the response of this structure contains two pass bands, but each pass band will have an nth order Chebyshev response.
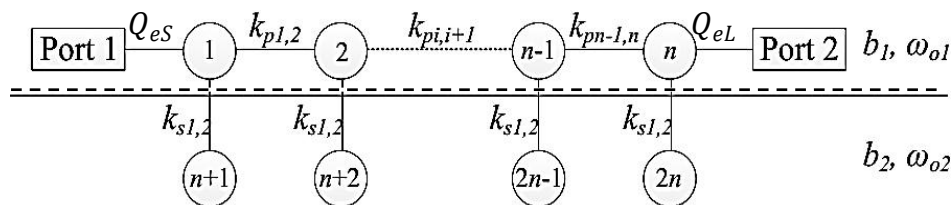

Fig. 3. Coupling resonators model for 2n[th] order dual-band filter using dual mode resonators.

Fig. 4 shows the equivalent circuit of the structure shown in Fig. 3, this circuit is labeled by the interim parameters and J-inverters (admittance inverters) connected to the band-pass resonators. Among the interim parameters, b_1 and ω_{01} describe the band-pass resonators (resonators from 1 to n), while b_2 and ω_{02} describe the band-stop resonators (resonators from $n + 1$ to $2n$). In the following, the method of finding the coupling matrix and the equivalent circuit elements of the dual-band filter is explained.
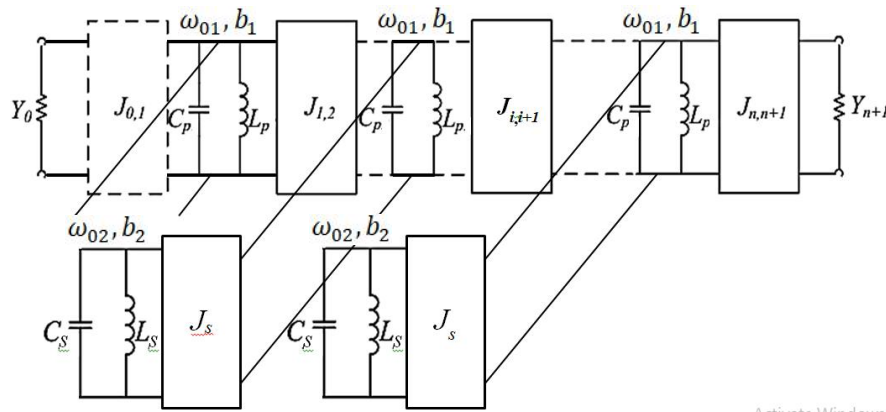
Fig. 4. Equivalent circuit model for the dual-band filter.

In Fig. 3, the circles represent the resonators, while the solid lines between them represent the coupling between the resonators. The two terminal resonators are connected to the input and output ports by the admittance inverters J_{01} and $J_{n,n+1}$ shown in the equivalent circuit in Fig. 4, and represented by the external quality factors Q_{eS} and Q_{eL} at the input and output in Fig. 3. Each of the band-pass resonators is coupled with a band-stop one forming what is called dual-resonance frequency resonator. In Fig. 4, Y_0 and Y_{n+1} represent the normalized admittances at input and output. $J_{i,i+1}$ represents the value of the admittance inverter between the ith and $(i+1)^{th}$ resonators, while J_s represents the value of the admittance inverter between each of the band-pass resonators and the corresponding band-stop resonator. The response of the part above the dashed line in Fig. 3 forms the response of all-pole Chebyshev response, while the resonators below the dashed line form the stop band between the two pass bands of the filter.

Equivalent Circuit Elements:

The values of the admittance inverter $J_{i,i+1}$ ($i = 0, \ldots, n+1$) in the equivalent circuit can be obtained from the all-pole Chebyshev design procedure using the following relations [20]:

$$J_{01} = \sqrt{\frac{Y_o}{g_0 \cdot g_1}}, \tag{22}$$

$$J_{i,i+1} = \sqrt{\frac{1}{g_i \cdot g_{i+1}}}, \tag{23}$$

$$J_{n,n+1} = \sqrt{\frac{Y_o}{g_n \cdot g_{n+1}}}, \tag{24}$$

$$J_s = 1, \tag{25}$$

where g_i's are the low pass prototype elements [20]. The remaining values of the equivalent circuit elements (inductors and capacitors) are given by:

$$b_i = \omega_{0i} \cdot C_i, \qquad ; \quad i = \begin{cases} p \ or \ s \ for \ C_i \ and \ L_i \\ 1 \ or \ 2 \ for \ b_i \ and \ \omega_i \end{cases} \tag{26}$$

where,

$$\omega_{0i} = \frac{1}{\sqrt{L_i \cdot C_i}}, \qquad ; \quad i = p \ or \ s \tag{27}$$

Elements of the Coupling Matrix:

The coupling matrix of the proposed dual-band filter can be written as:

$$M = \begin{bmatrix} M_p & M_{ps} \\ M_{ps} & M_s \end{bmatrix}. \tag{28}$$

That is, it consists of a structure of four matrices, each of which is defined as [20], [21]:

$$M_p = \begin{bmatrix} k_{1,1} & k_{1,2} & \cdots & 0 \\ k_{1,2} & k_{2,2} & \cdots & \vdots \\ \vdots & \vdots & \ddots & k_{n,n-1} \\ 0 & \cdots & k_{n-1,n} & k_{n,n} \end{bmatrix}, \quad \text{where;} \begin{cases} k_{i,i} = \dfrac{\omega_0}{\omega_{01}} - \dfrac{\omega_{01}}{\omega_0} \\ k_{i,i+1} = k_{i+1,i} = \dfrac{1}{b_1\sqrt{g_i g_{i+1}}} \end{cases} \tag{29}$$

$$M_s = \begin{bmatrix} k_{n+1,n+1} & 0 & \cdots & 0 \\ 0 & \ddots & & \vdots \\ \vdots & & \ddots & 0 \\ 0 & \cdots & 0 & k_{2n,2n} \end{bmatrix}, \qquad \text{where;} \ k_{i,i} = \dfrac{\omega_0}{\omega_{02}} - \dfrac{\omega_{02}}{\omega_0} \tag{30}$$

$$M_{ps} = \begin{bmatrix} k_{1,1} & 0 & \cdots & 0 \\ 0 & \ddots & & \vdots \\ \vdots & & \ddots & 0 \\ 0 & \cdots & 0 & k_{n,n} \end{bmatrix}, \qquad \text{where;} \ k_{i,i} = \dfrac{1}{\sqrt{b_1 b_2}} \tag{31}$$

where,

$$\omega_0 = \sqrt{\omega_{L1} \cdot \omega_{H2}}. \tag{32}$$

While, the input and output external quality factors are given by: [20]

$$Q_{eS} = \frac{b_1}{J_{01}^2} = b_1 \cdot g_0 \cdot g_1, \tag{33}$$

$$Q_{eL} = \frac{b_1}{J_{n,n+1}^2} = b_1 \cdot g_n \cdot g_{n+1}. \tag{34}$$

where; J_{01} and $J_{n,n+1}$ are given by (22) – (24).

Dual-Band Filter Response:

Having found the equivalent circuit and the coupling matrix elements, the filter response can be found either by simulating the equivalent circuit in circuit simulation software such as ADS or MW office or other software used in microwave circuit simulation, or using the coupling matrix. The response of the filter is given by [9], [20]:

$$S_{21} = \frac{2}{\sqrt{Q_{eS} \cdot Q_{eL}}} \cdot [A]_{n1}^{-1}, \tag{35}$$

$$S_{11} = \mp \left(1 - \frac{2}{Q_{eS}} \cdot [A]_{11}^{-1} \right), \tag{36}$$

where A is the admittance matrix of the equivalent circuit [9], [20] which is given by:

$$[A] = [q] + D[U] - j[M] , \tag{37}$$

where $[M]$ is the coupling matrix whose elements are given by (28) – (31), $[U]$ is the identity matrix and D is the frequency transformation (i.e. the relation (6)), and $[q]$ is the quality matrix with all of its entries are equal to zero except for the first element of the main diagonal, which is equal to the invert of the quality factor at the input, i.e. $\frac{1}{Q_{eS}}$, and the last element of the main diagonal, which is equal to the invert of the quality factor at the output i.e. $\frac{1}{Q_{eL}}$, and they are given by (33) and (34).

III. VERIFYING THE SYNTHESIS PROCEDURE AND THE TRANSFORMATION FORMULA

In this section a dual-band pass filter is designed with the following specifications:

- The filter is of 10th order, i.e. 5th order Chebyshev response for each pass band

- Pass bands (the return loss within the pass bands is needed to be below -20 dB):

   The first passband frequency range [8 – 9.575] GHz.

   The second passband frequency range [10.05 - 11] GHz.

- Technology: Interdigital Filter

A. Verifying the Frequency Transformation

The frequency transformation is first verified. The frequency transformation is applied to the 5th order Chebyshev response, where the transmission coefficient S_{21} and the return loss S_{11} are given by relations (3) and (4). By performing the frequency transformation represented in relation (7) on the transmission and return loss coefficients (3) and (4) directly using MATLAB software, the response shown in Fig. 5 is obtained. It is clear from the figure that the response fulfills the required specifications of the filter.

B. Verifying the Equivalent Circuit Model

Using the equivalent circuit model given in Fig. 4 (relation (22) through (27)), the equivalent circuit of the dual-band filter is found as shown in Fig. 6. Where; Fig. 6 shows the equivalent circuit model with the values of the circuit elements (the values of capacitors and inductors in addition to the admittance inverters). The circuit is simulated using the MW Office software. Fig. 7 shows the simulation results. We also note that this result is completely identical to the result shown in Fig. 5. This congruence is intuitive since the values of the equivalent circuit elements are considered precisely.
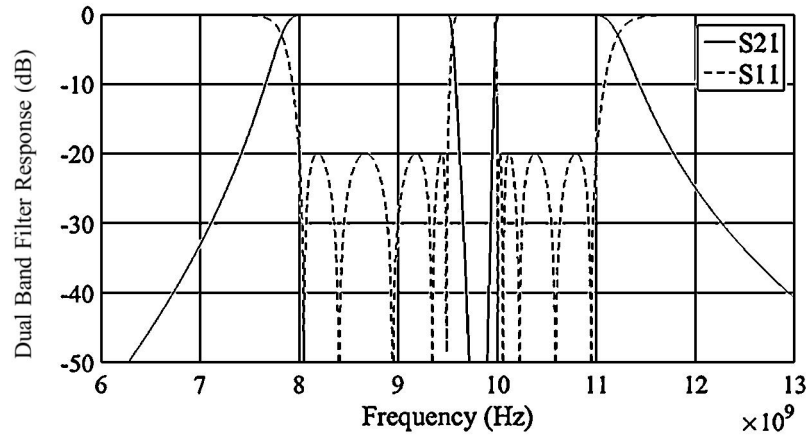
Fig. 5. The response obtained from frequency transformation from the low pass prototype domain to dual-band one.
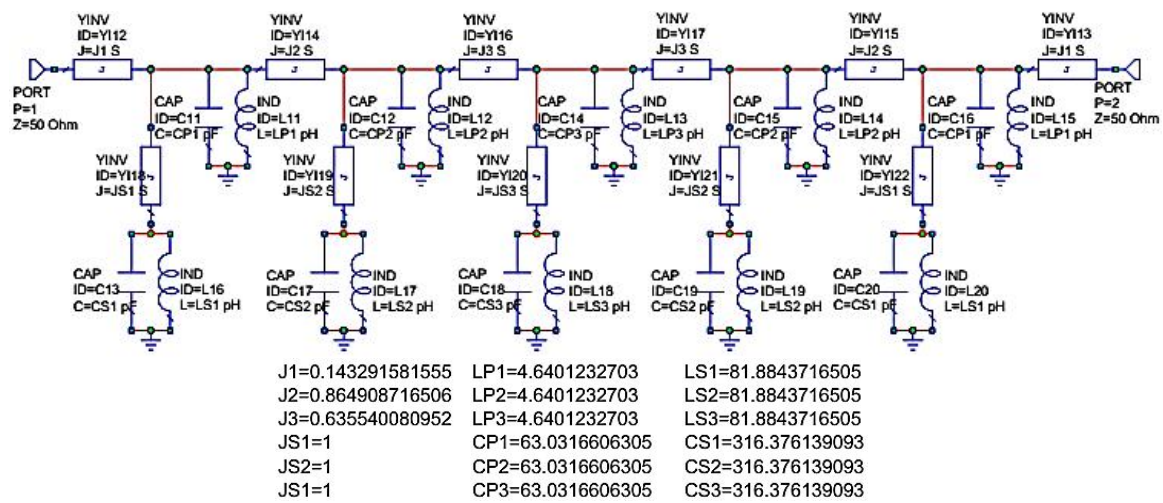

J1=0.143291581555	LP1=4.6401232703	LS1=81.8843716505
J2=0.864908716506	LP2=4.6401232703	LS2=81.8843716505
J3=0.635540080952	LP3=4.6401232703	LS3=81.8843716505
JS1=1	CP1=63.0316606305	CS1=316.376139093
JS2=1	CP2=63.0316606305	CS2=316.376139093
JS1=1	CP3=63.0316606305	CS3=316.376139093

Fig. 6. The equivalent circuit of the considered dual-band filter.

C. Verifying the Coupling Matrix

Using (28) – (31), the coupling matrix of the dual-band filter is obtained to be as:

$$
M = \begin{bmatrix}
-0.0146 & 0.2322 & 0 & 0 & 0 & 0.1228 & 0 & 0 & 0 & 0 \\
0.2322 & -0.0146 & 0.1706 & 0 & 0 & 0 & 0.1228 & 0 & 0 & 0 \\
0 & 0.1706 & -0.0146 & 0.1706 & 0 & 0 & 0 & 0.1228 & 0 & 0 \\
0 & 0 & 0.1706 & -0.0146 & 0.2322 & 0 & 0 & 0 & 0.1228 & 0 \\
0 & 0 & 0 & 0.2322 & -0.0146 & 0 & 0 & 0 & 0 & 0.1228 \\
0.1228 & 0 & 0 & 0 & 0 & 0.0912 & 0 & 0 & 0 & 0 \\
0 & 0.1228 & 0 & 0 & 0 & 0 & 0.0912 & 0 & 0 & 0 \\
0 & 0 & 0.1228 & 0 & 0 & 0 & 0 & 0.0912 & 0 & 0 \\
0 & 0 & 0 & 0.1228 & 0 & 0 & 0 & 0 & 0.0912 & 0 \\
0 & 0 & 0 & 0 & 0.1228 & 0 & 0 & 0 & 0 & 0.0912
\end{bmatrix}
\qquad (38)
$$

By applying relation (35) and (36) using MATLAB, the response shown in Fig. 8 is obtained. These results coincide with the simulation and the equivalent circuit ones shown in Fig. 6 and 7 respectively. This is self-evident since the coupling matrix forms a mathematical model of the filter that leads to an accurate result in terms of response.
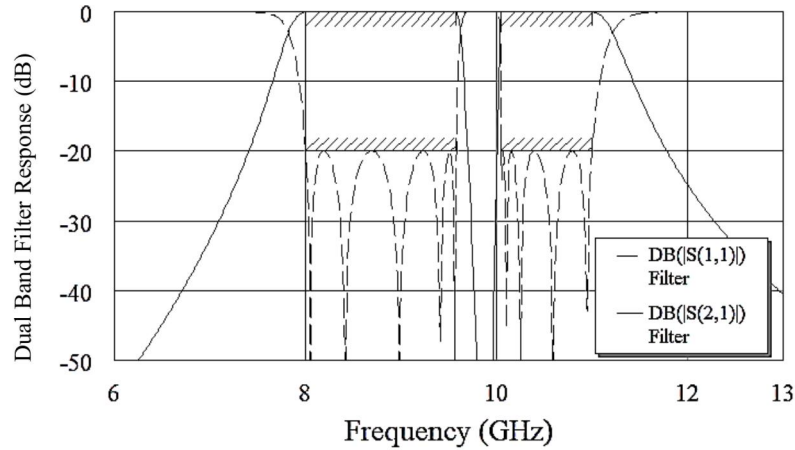
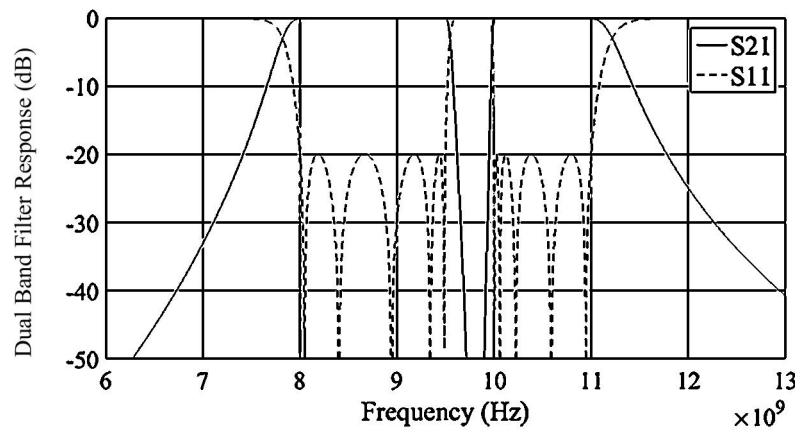Fig. 7. The response of the equivalent circuit shown in Fig. 6.

Fig. 8. The response obtained from the coupling matrix of the considered dual-band filter.

IV. FILTER DESIGN AND IMPLEMENTATION

A design procedure of filters based on coupling matrix is adopted in constructing the dual-band filter in this section. Using the coupling matrix (38), the physical dimensions of the filter is obtained. Fig. 9(a) shows the 3D view of the designed and simulated dual band filter using CST Microwave Studio, and Fig. 9(b) shows the top view of the same designed and simulated filter. After having got the full physical dimensions of the dual-band filter, we rounded some dimensions to the nearest hundred micrometers, such as the distances between the resonators, the height of the input and output connectors, the distance between the two terminal resonators and the walls adjacent to them, and the height of the resonators. Then we simulated the filter using FD Solver simulator in CST. The simulation results are the indicated curves (Before Tuning) shown in Fig. 10. Fig. 10 also shows the filter's response after a simple tuning of the fine-tuning screws; this response is indicated by (tuned). We note that the response is close to the specifications of the required filter, in terms of the pass bands and stop band in addition to the return loss, given in Fig. 5. The difference between the simulation result before and after the tuning results from our approximations of some physical dimensions. But

by performing the tuning, we notice that the filter specifications are very close to the required ones (the width of the two pass bands, the width of the stop band, and the return loss within the pass bands).
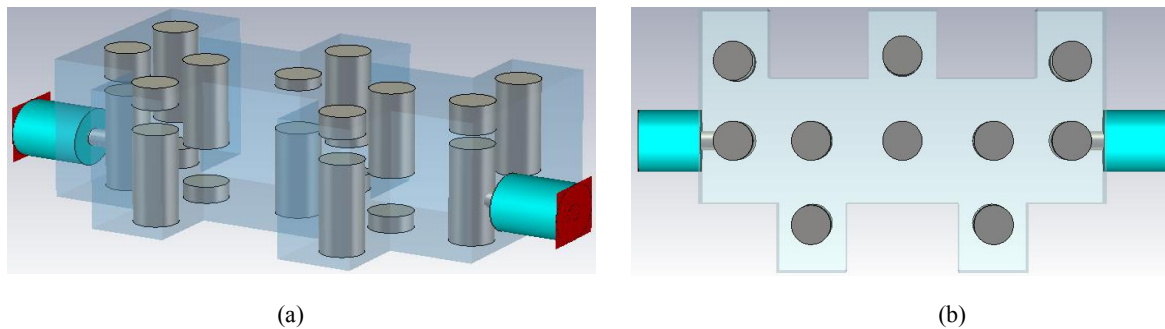

(a)   (b)
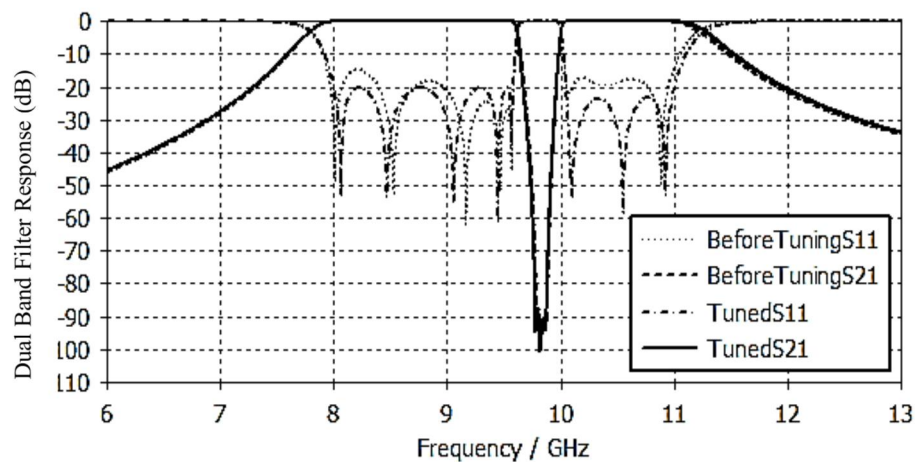
Fig. 9. The obtained Interdigital filter, (a) 3D view, (b) top view.

Fig. 10. The response of the designed interdigital filter.

Fig. 11 shows the shape of the response within the pass bands, and shows the amount of ripple within them, which is approximately less than 0.0436 dB. From this response, we can also see that the ripple obtained from the simulation achieves the desired one, which corresponds to the values of S_{11} within the pass band denoted "TunedS11" in Fig. 11 (below -20dB) over the two pass bands.
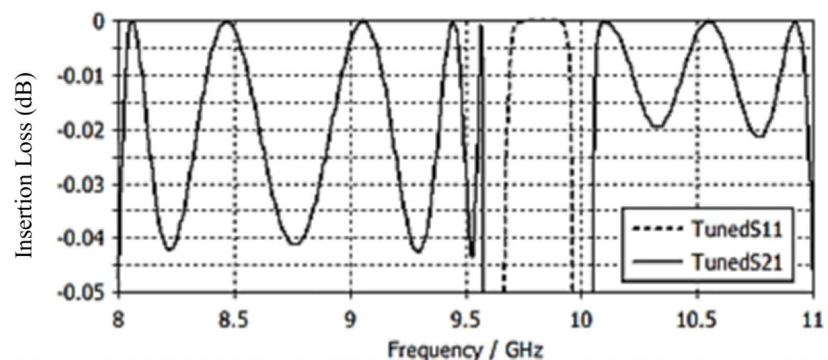

Fig. 11. Zoom of the designed filter's response in the pass bands.

The designed and simulated filter is implemented. Fig.12 shows the filter assembly parts fabricated to construct the filter. These parts have been fabricated using the commercial alloyed aluminum. After

364

assembling the filter, it had the photo shown in Fig. 13. The filter was measured using a Scalar Network Analyzer. Fine tuning (using the tuning screw) was performed to obtain the resulting response shown in Fig.14. In order to verify the design, the simulation results of the filter are also shown in Fig.14. It's clear, from Fig.14, that excellent agreement between the simulation and the measurement is observed (in terms of the width of the two pass bands, the width of the stop band, and the return loss within the pass bands). More insertion loss in the response of the fabricated filter was observed from the measurement. This insertion loss is caused by the losses of the aluminum material and the losses of the SMA connectors used for the filter. We also note that the insertion loss is greater on both edges of the two pass bands close to the stop band, which reaches about 2dB. Fig. 14(a) shows these differences in insertion loss between measurement, simulation and analytical results.

As can be seen from Fig. 15(b), the fabricated filter meet the required return loss in the second pass band, while about 2dB between the return loss of the fabricated filter and the return loss in the analytical or simulation results is observed in the first pass band.

Comparing the simulation or measurement results with the theoretical ones (Fig. 15(c)), we can notice that the selectivity within the stop band between the two pass bands is very good, although the designed filter did not achieve the selectivity outside the whole band of the filter (between the upper edge of the higher band and the lower edge of the lower band). Also, a little frequency shift of the stop band is noticed.

Comparing with some of the works that were mentioned in some recent scientific references, we can note that the required specifications of the designed filters are approximately achieved in [2], [7], while S_{11} in [2] doesn't meet the required value, although the value of S_{11} adopted in [2] was -15dB compared to -20dB in the case of the designed filter presented in this paper. While the required specifications of the filter in [7] are met in terms of the required pass-bands, however, the filter obtained in [7] showed poor selectivity compared to the filter presented in this paper, especially in the stop band between the two pass bands.
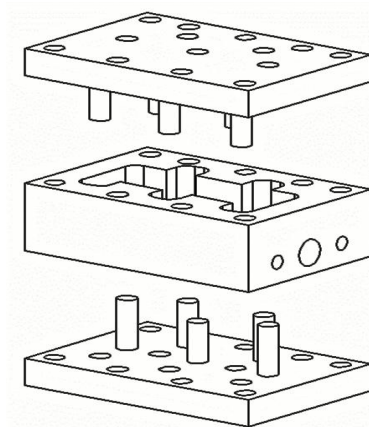

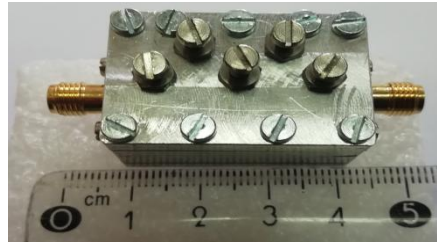Fig. 12. Assembly parts for the fabricated dual-band filter.

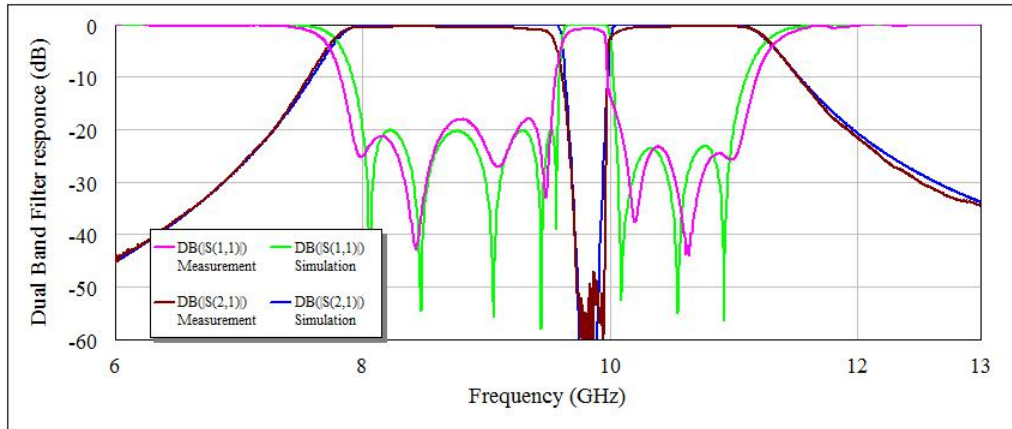Fig. 13. Photo for the fabricated dual-band filter.

Fig. 14. simulation and measurement results for the designed and fabricated dual-band. filter.
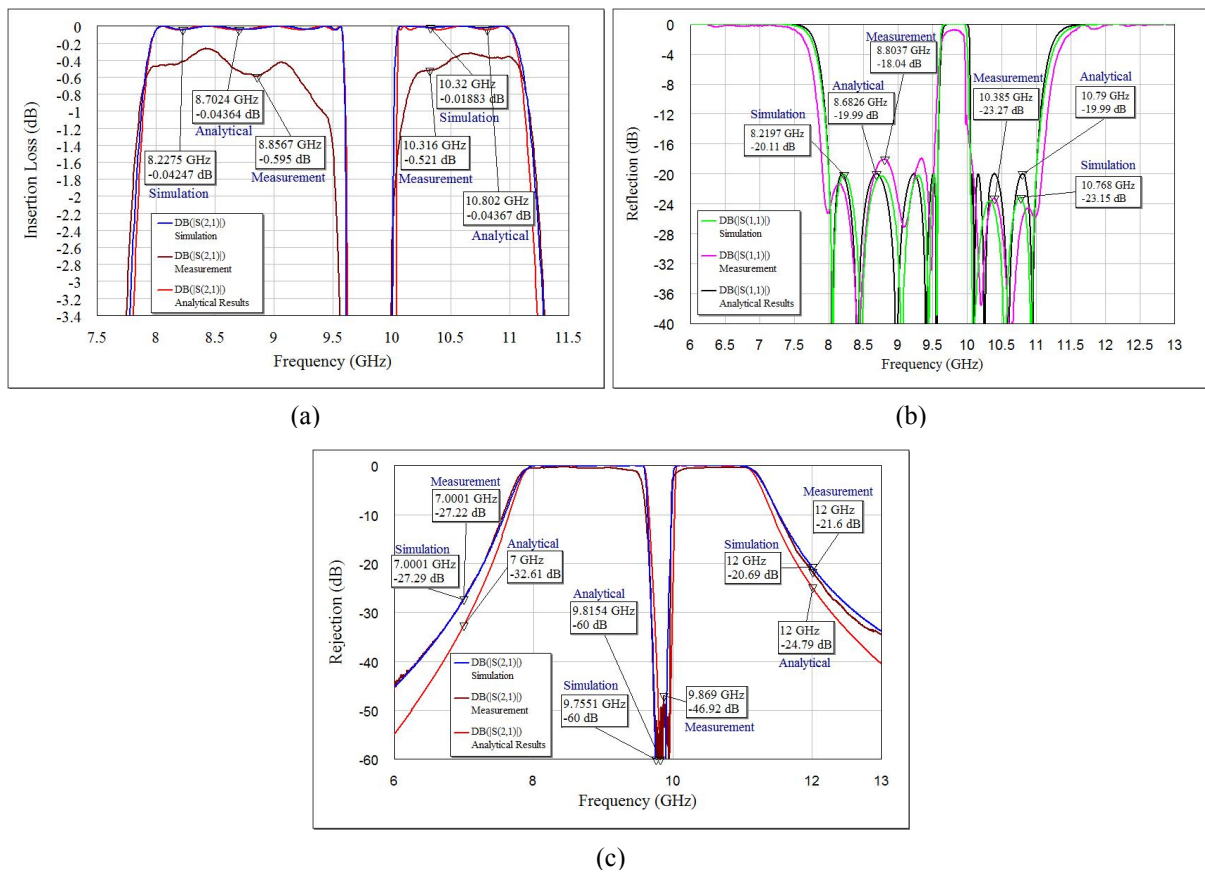

(a)

(b)

(c)

Fig. 15. Comparison between analytical, simulation and measurement results. (a) Demonstration of insertion loss of the filter, (b) Demonstration of return loss of the filter, (c) Demonstration of rejecion of the filter.

V. CONCLUSION

In this article, an analytical methodology for designing a dual-band filter has been used benefiting from frequency transformation between the normalized frequency domain of low-pass prototype, and the real frequency domain of the filter. The adopted method was purely analytical in the process of finding the coupling matrix that fulfills the required filter specifications, without having to perform numerical optimization on the coupling matrix in order to obtain the response of the two pass bands. The procedure also found the equivalent circuit for this type of filters, which includes connecting each of the primary resonators (a band-pass resonator) of the filter to a resonator responsible for the stop band (a band-stop resonator) in order to form dual-resonance frequency resonators. The frequency transformation formula is verified through an example. The equivalent circuit and the coupling matrix are also analytically deduced through the same example. Using electromagnetic structures simulator, the interdigital dual-band filter is designed and simulated. The simulation results fulfill the specifications of the given filter example, and show the possibility of achieving the required frequency response specifications of the filter. The designed and simulated filter is implemented and measured using a Scalar Network Analyzer. Measurement results confirm the simulation results and the efficiency of the synthesis procedure.

REFERENCES

[1] FCC, Washington, "DC, Federal Communications Commission revision of Part 15 of the Commission's rules regarding ultra-wideband transmission systems," First Report Order FCC 2, vol. 48, 2002.
[2] Y. Leong, S. Cheab, S. Soeung, and P. W. Wong, "A New Class of Dual-Band Waveguide Filters Based on Chebyshev Polynomials of the Second Kind," *IEEE Access*, vol. 8, pp. 28571–28583, 2020.
[3] Y. X. Wang, Y. L. Chen, W. H. Zou, W. C. Yang, and J. Zen, "Dual-Band Bandpass Filter Design Using Stub-Loaded Hairpin Resonator and Meandering Uniform Impedance Resonator," *Progress In Electromagnetics Research Letters*, vol. 95, pp. 147–153, 2021.
[4] M. H. Weng, F. Z. Zheng, H. Z. Lai and S.-K. Liu, "Compact Ultra-Wideband Bandpass Filters Achieved by Using a Stub-Loaded Stepped Impedance Resonator," *Electronics*, vol. 9, np. 2, pp. 209, 2020.
[5] P. Zhang, L. Liu, D. Chen, M. H. Weng and R. Y. Yan, "Application of a Stub-Loaded Square Ring Resonator for Wideband Bandpass Filter Design," *Electronics*, vol. 9, no. 1, pp. 176, 2020.
[6] A. Lalbakhsh, A. Ghaderi, W. Mohyuddin, R. B. B. Simorangkir, N. B. Makou, M. S. Ahmad, G. H. Lee and K. W. Kim, "A Compact C-Band Bandpass Filter with an Adjustable Dual-Band Suitable for Satellite Communication Systems," *Electronics*, vol. 9, no. 7, pp. 1088, 2020.
[7] K. Yoon and K. *Kim*, "Design of Dual Ultra–Wideband Band–Pass Filter Using Stepped Impedance Resonator λg/4 Short Stubs and T–Shaped Band-Stop Filter," *Electronics*, vol. 10, no. 16, pp. 1951, 2021.
[8] M. Faisal, S. Khalid, M. U. Rehman, and M. A. Rehman, "Synthesis and Design of Highly Selective Multi-Mode Dual-Band Bandstop Filter," *IEEE Access*, vol. 9, pp. 43316–43323, 2021.
[9] R.J. Cameron, C.M. Kudsia and R.R. Mansour, *Microwave Filters for Communication Systems : fundamentals, design, and applications*, John Wiley & Sons, 2018.
[10] Y. Wu, E. Fourn, P. Besnier and C. Quendo, "Direct Synthesis of Quad-Band Band-Pass Filter by Frequency Transformation Methods," In 2019 49th *European Microwave Conference* (EuMC), 2019, pp. 196-199.
[11] R. Levy, "Generalized rational function approximation in finite intervals using Zolotarev functions," *IEEE Transactions on Microwave Theory and Techniques*, vol. 18, no. 12, pp. 1052–1064, 1970.
[12] H. C. Bell, "Zolotarev bandpass filters," *IEEE transactions on microwave theory and techniques*, vol 49, no. 12, pp. 2357–2362.
[13] A. Mohan1, S. Singh and A. Biswas, "Generalized Synthesis and Design of Symmetrical Multiple Passband Filters," *Progress In Electromagnetics Research B*, vol. 42, pp. 115–139, 2012.
[14] Y. T. Kuo, J. C. Lu, C. K. Liao, and C.-Y. Chang, "New Multiband Coupling Matrix Synthesis Technique and its Microstrip Implementation," *IEEE Transactions on Microwave Theory and Techniques*, vol. 58, no. 7, pp. 1840–1850, 2010.
[15] L. Gang, "Coupling Matrix Optimization Synthesis for Filters with Constant and Frequency-Variant Couplings," *Progress In Electromagnetics Research Letters*, vol. 82, pp. 73–80,2019.

[16] L. C. Tsai and C. W. Hsue, "Dual-band bandpass filters using equal length coupled-serial-shunted lines and Z-transform technique," *IEEE Transactions on Microwave Theory and Techniques*, vol. 52, no. 4, pp. 1111–1117, 2004.

[17] G. Macchiarella and S. Tamiazzo, "A design technique for symmetric dual-band filters," In *IEEE MTT-S International Microwave Symposium Digest, 2005*, pp. 115–118, 2005.

[18] G. Macchiarella and S. Tamiazzo, "Design techniques for dual-passband filters," *IEEE Transactions on Microwave Theory and Techniques*, vol. 53, no. 11, pp. 3265–3271, 2005.

[19] A. G. Lampérez and M. S. Palma, "Single-Band to Multiband Frequency Transformation for Multiband Filters, " *IEEE Transactions on Microwave Theory and Techniques*, vol. 59, no. 12, pp. 3048–3058, 2011.

[20] J. S. Hong, and M. J. Lancaster. *Microstrip Filters for RF/Microwave Applications*. John Wiley and Sons, United Kingdom, 2001.

[21] G. L. Matthaei, L. Young, and E.M.T. Jones. *Microwave filters, impedance- matching networks, and coupling structures*. *Volume 2*. Stanford Research Inst Menlo Park CA, 1963.